

Preparation and utilization of TiO₂ supported on Zeolite Y as a photocatalyst for solar light degradation of aqueous phenolic compounds



Engineering

KEYWORDS : TiO₂/zeolite catalyst; solar light photocatalysis; phenol; 2-chlorophenol; 4-chlorophenol

Purabi Mahanta

Department of Chemistry, Gauhati University, Guwahati 781014, Assam, India

Krishna G Bhattacharyya

Department of Chemistry, Gauhati University, Guwahati 781014, Assam, India

ABSTRACT

In this work, the solar radiation induced photocatalytic degradation of phenol, 2-chlorophenol and 4-chlorophenol was studied over a model catalyst prepared by supporting titanium dioxide on zeolite Y. The catalyst characterization was done by techniques like XRD, FTIR and SEM. The effects of various parameters like catalyst loading, initial concentration of the dye, reaction time and pH were investigated. The efficiencies of the catalyst calcined at 773 K were compared with those of the uncalcined catalyst, the original titanium dioxide, and the parent zeolite Y. After a reaction was over, the reaction mixture was centrifuged and the unconverted reactant was estimated spectrophotometrically in supernatant. The used catalysts were washed thoroughly and were tested for reuse capability. The catalysts could be reused up to four runs without much loss of activity. The reactions were also carried out in the dark and the results were compared with those of the solar experiments. The progress of the reactions was also monitored by measuring the chemical oxygen demand of the reaction mixture from time to time. The reaction kinetics was worked out.

1. Introduction

Improper waste disposal practices have resulted in contamination of various environmental media. Phenol and chlorophenols, identified by the US EPA (Environmental Protection Agency) as priority pollutants represent one of the most abundant families of industrial toxic compounds. They are harmful to human health and ecosystem even at low concentrations. Phenol and chlorophenols, apart from direct entry from various chemical industries, are also generated as degradation byproducts of a variety of agrochemicals such as herbicides and pesticides. Conventional treatment technologies, such as air stripping, carbon adsorption and biological treatment etc. have limitations in removing these persistent refractory organic compounds from wastewater. Therefore, various advanced wastewater treatment technologies have been developed over the last 20 years [1-7]. Heterogeneous photocatalysis using semiconductors is one of the most promising technologies among them [8-10]. When the photocatalysis is carried out utilizing sunlight as the source of energy, which is free and inexhaustible, the possibilities are immense.

Among various semiconducting materials, TiO₂ has attracted the most attention because of its high photocatalytic activity, resistance to photocorrosion, low cost, non-toxicity and favourable band-gap energy [11]. Anatase phase of TiO₂ is more active than the rutile phase [11-13]. However TiO₂ has a tendency to aggregate in aqueous suspension due to its small size. Formation of large particles reduces surface area and pore volume and reduces the catalytic efficiency rapidly. Coarse particles also increase turbidity of the reaction mixture decreasing solar light penetration. Thus, it is difficult to maintain the rate of photocatalytic transformation if TiO₂ is used alone. Moreover it is very difficult to separate pure TiO₂ powder from water when used in aqueous system making the recovery of the catalyst from the reaction mixture very difficult. These difficulties are sought to be overcome in this work by using a large area support on which TiO₂ particles are dispersed.

According to previous reports, it is very important that the target compound is adsorbed enough on the TiO₂ surface before photocatalytic decomposition. The enrichment of organic pollutants also greatly facilitates the photodegradation efficiency and reduces the electron-hole recombination process on the surface of TiO₂ [14-15]. Therefore, extensive research has been going on to develop techniques to enhance the adsorption ability of the photocatalyst without affecting its photocatalytic activity in a suspension [16-22]. Among various supports used for TiO₂

photocatalysts, zeolites have drawn attention due to their large surface areas, internal pore volume, unique uniform pores, channel size, photochemical stability, and chemical inertness [23-25]. In the present work, solar photodegradation of three model compounds, namely phenol, 2-chlorophenol (2-CP) and 4-chlorophenol (4-CP) were studied over TiO₂ supported on zeolite Y catalyst.

2. Experimental

2.1. Materials used

Zeolite Y (Sodium form) was obtained from HiMedia Laboratories Pvt. Ltd, Mumbai, India, and titanium dioxide was obtained from E. Merck, Mumbai, India. Phenol, 2-CP and 4-CP for the reactions were procured from E. Merck, Mumbai, India, Merck-Schuchardt, Hohenbrunn, Germany and Fluka, Switzerland respectively. All other chemicals used were of analytical grade.

2.2. Catalyst Preparation

Two different suspensions were prepared by taking equal amounts (by weight) of TiO₂ and zeolite Y in a large volume of distilled water under continuous stirring. The TiO₂ suspension was added to the zeolite Y suspension with vigorous stirring. Stirring was continued for 24 hours. The resulting material was centrifuged, washed with double-distilled water several times, dried in hot air oven at 393 K for 8 h, and then calcined at 773 K for 24 h. The prepared catalysts were preserved in stoppered glass bottles.

2.3. Catalyst Characterisation

XRD patterns of the catalysts were recorded in reflection mode (Cu K α radiation, $\lambda = 1.5406 \text{ \AA}$) on a Bruker D8 Advance diffractometer in the 2θ range of 10° to 80° with a step size of 0.019917° . The FTIR spectra of catalysts were taken by Perkin-Elmer Spectrum RXI spectrophotometer (range 4000 - 450 cm^{-1}) using KBr self-supported pellet technique. The SEM images of the catalysts were recorded with a scanning electron microscope (JEOL JSM-6360).

2.4. Reaction Study

All the solar experiments were conducted under direct sunlight in the month of July during the daylight hours of 10 to 15 h. The variation of solar intensity during the experiment was recorded with a digital luxmeter (HTC) which can measure intensity in the range of $1 - 1 \times 10^5 \text{ Lux}$. The sensor was always set in the position of maximum intensity and the solar light intensity was measured every 5 min during the duration of the reaction. The variation in solar intensity with time, plotted for three consecu-

five days, is shown in Fig.1. From the figure it is clear that the variation in solar intensity is minimum across the days. The average light intensity was around 109000 lx. For comparison of the photocatalytic activity of the prepared catalysts with the parent compounds, experiments were conducted simultaneously to avoid fluctuations in solar intensity.

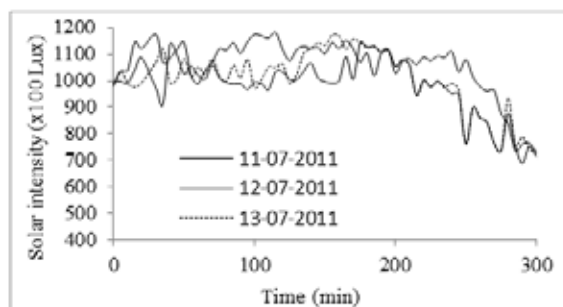


Fig.1. Solar intensity variation with time plotted for three consecutive days

The reaction mixture taken in 250 ml round bottom flask was stirred vigorously using a magnetic stirrer for the entire time span of the experiment. The reaction mixture was stirred in complete dark for 30 min prior to the start of the solar experiments to eliminate the changes due to adsorption. After the reaction was over, the mixture was centrifuged at 8000 rpm (Remi Research Centrifuge) and the unconverted portion of the reactant was determined in the supernatant layer spectrophotometrically (Hitachi UV-visible U3210). The percentage of conversion was computed by using the following expression:

$$\% \text{ conversion} = (\text{Co} - \text{Ct}) \times 100 / \text{Co}$$

where, Co (mol L⁻¹) and Ct (mol L⁻¹) are reactant concentrations before and after reaction for time t (min).

COD was determined by using the open reflux method (APHA, 1989). In this method a sample was refluxed for 2 h with strongly acid solution with a known excess of potassium dichromate (K₂Cr₂O₇) and K₂Cr₂O₇ remaining unutilized was titrated with ferrous ammonium sulphate (FAS). The end point was indicated by the first sharp colour change from blue green to reddish brown. A blank containing the reagents and volume of distilled water equal to the sample taken was refluxed and titrated in the similar manner. COD of the samples is determined using the following formula:

$$\text{COD as mg O}_2/\text{L} = (\text{A} - \text{B}) \times \text{M} \times 8000 / \text{mL of sample taken}$$

where A = mL of FAS used for blank, B = mL of FAS used for sample and M = molarity of FAS. The COD removal efficiency of the catalyst was calculated as % COD removed using the following formula

$$\% \text{ COD removed} = (\text{COD}_i - \text{COD}_f) / \text{COD}_i \times 100 \%$$

where COD_i = COD before reaction and COD_f = COD after reaction

3. Results and discussion

3.1. XRD studies

XRD patterns of the prepared catalysts, parent TiO₂ and that of parent zeolite Y were recorded in 2 θ range of 10 to 80 $^\circ$. The observed XRD patterns are given in Fig. 2. The parent TiO₂ has a prominent peak at 2 θ = 25.39 $^\circ$ (d = 3.5 Å) followed by peaks at 2 θ values of 37.04 $^\circ$ (d = 2.43 Å), 37.90 $^\circ$ (d = 2.37 Å), 38.65 $^\circ$ (d = 2.33 Å), 48.14 $^\circ$ (d = 1.89 Å), and 53.97 $^\circ$ (d = 1.69 Å), 55.15 $^\circ$ (d = 1.66 Å), 62.78 $^\circ$ (d = 1.48 Å), 68.85 $^\circ$ (d = 1.36 Å), 70.34 $^\circ$ (d = 1.34 Å), and 75.10 $^\circ$ (d = 1.26 Å). These peaks can be attributed to

101, 103, 004, 112, 200, 105, 211, 204, 116, 220 and 215 diffraction planes respectively. It was observed that only anatase crystalline phase is present. The background of the XRD pattern is flat indicating that TiO₂ is crystalline. The parent zeolite Y gave XRD peaks at 2 θ values of 10.12, 12.42, 15.16, 20.37, 21.61, 23.94, 30.75 and 34.11 $^\circ$ corresponding to d spacings of 8.73, 7.12, 5.84, 4.35, 4.11, 3.71, 2.91 and 2.63 Å respectively. The obtained diffraction pattern matches well with those available in the literature [23].

A comparison of the XRD patterns of the prepared photocatalysts (both uncalcined and calcined at 773 K) with those of parent TiO₂ and zeolite Y revealed that the prepared catalysts exhibited crystallinity similar to those of the parent compounds. The peak positions and the d-spacings of the peaks corresponding to the parent compounds remained nearly same on the prepared photocatalysts. This indicates no change in the interlayer distance. The intensity of both TiO₂ and zeolite Y peaks in the prepared photocatalysts decreased in comparison to the parent compounds. Intensities of the peaks were found to have increased after calcination in comparison to the uncalcined TiO₂-zeolite Y.

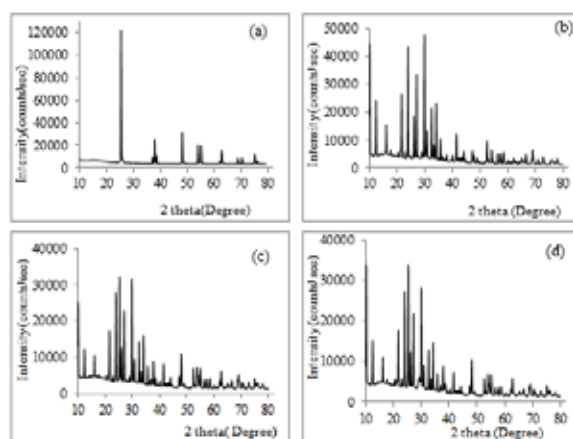
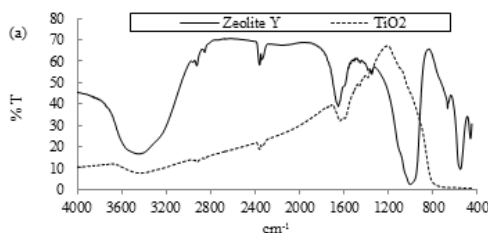


Fig. 2: XRD patterns of (a) parent TiO₂ (b) parent zeolite Y (c) uncalcined TiO₂-zeolite Y (d) calcined TiO₂-zeolite Y

3.2. IR spectroscopy

Fig. 3 shows the FTIR spectra of the prepared TiO₂-zeolite Y (both uncalcined and calcined at 773 K) in the frequency range 400 – 4000 cm⁻¹. FTIR spectra of pure, untreated TiO₂ and zeolite Y are also given in Fig. 3 for comparison. The absorption bands at 704 – 695 cm⁻¹ correspond to internal tetrahedral symmetric stretching and bands at 573 - 575 cm⁻¹ are due to double ring (external vibrations of tetrahedral linkages) [26]. TiO₂-zeolite Y catalyst retained the prominent peaks in the IR adsorption spectra after calcination. The broad band near 3400 cm⁻¹ can be attributed to the stretching H–O–H vibrations and the band around 1600 cm⁻¹ corresponds to the bending vibration of H–O–H group. After calcination at 773 K, a decrease in the intensity of these bands was observed. These bands indicate the presence of tightly bound water to the anatase surface [11].



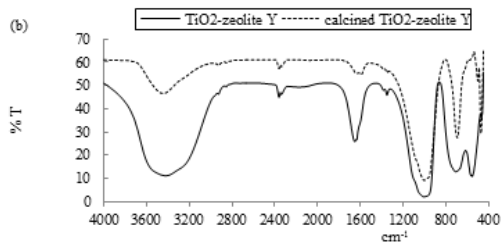


Fig. 3. FTIR spectra of (a) parent TiO₂ and parent zeolite Y (b) uncalcined TiO₂-zeolite Y and calcined TiO₂-zeolite Y

3.3. Scanning electron microscopy (SEM) measurements

SEM micrographs of parent TiO₂, parent zeolite Y, TiO₂ supported on zeolite Y (uncalcined) and TiO₂ supported on zeolite Y (calcined at 773 K) are shown in Fig. 4. Small particles of almost uniform size were observed in the SEM micrograph of the parent TiO₂. Some agglomerations were also observed in the parent TiO₂. The zeolite Y particles are cubes with rounded edges and are of different sizes. It is observed that the shape and size of the zeolite particles remained same in the supported catalysts. The surface of the zeolite particles is observed to be uniformly covered with small TiO₂ particles in the SEM micrograph of TiO₂ supported on zeolite Y. No significant change could be observed due to calcination.

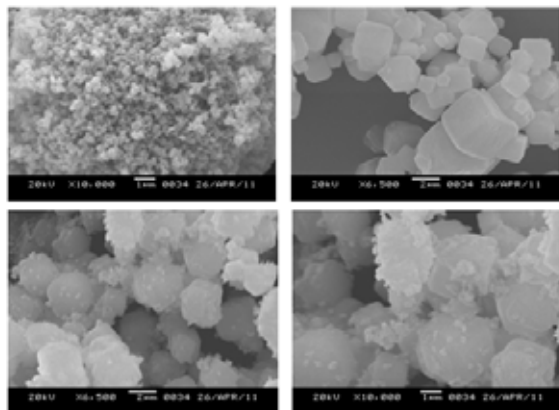


Fig. 4. SEM images of (a) parent TiO₂ (b) parent zeolite Y (c) uncalcined TiO₂-zeolite Y (d) calcined TiO₂-zeolite Y

3.4. Photocatalytic activity of TiO₂ supported on zeolite Y

Before investigating the effectiveness of the prepared photocatalysts, a set of blank experiments were carried out with the following systems:

1. Aqueous solution of phenol, 2-CP or 4-CP alone without any catalyst in complete dark
2. Phenol, 2-CP or 4-CP aqueous solution in absence of catalyst under sunlight
3. Phenol, 2-CP or 4-CP aqueous solution in presence of parent TiO₂ alone in complete dark
4. Phenol, 2-CP or 4-CP aqueous solution in presence of parent TiO₂ alone under sunlight
5. Phenol, 2-CP or 4-CP aqueous solution with parent zeolite Y alone in complete dark
6. Phenol, 2-CP or 4-CP aqueous solution with parent zeolite Y alone under sunlight
7. Phenol, 2-CP or 4-CP aqueous solution with TiO₂-zeolite Y as the catalyst in complete dark.

No measurable conversion could be recorded in (i) to (iii) and

conversions achieved in (v) to (vii) were very much less (< 10%), while only in (iv) a significant amount of degradation (~50%) was recorded. It is clear from these blank experiments that the aqueous solutions of phenol, 2-CP and 4-CP are quite stable and do not have any tendency for self-oxidation. They do not undergo any direct photolysis under solar radiation. zeolite Y is not photocatalytically active, but acts as an adsorbent only. TiO₂ have photocatalytic activity but lack good adsorption capacity. The prepared catalyst TiO₂-zeolite Y, show very little oxidative power with respect to phenol, 2-CP and 4-CP in absence of sunlight. It may be noted that TiO₂-zeolite Y was calcined at 773 K for 5 h before use. However, it was observed that when the catalysts were used without calcination, the conversions were only marginally lower (Fig. 5). For the sake of reproducibility, the results obtained with the calcined catalysts are only reported here.

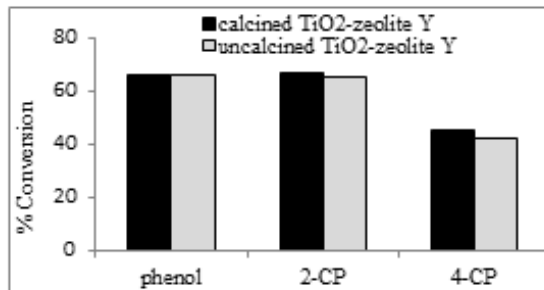


Fig.5. Comparison of the solar photodegradation of phenol, 2-CP and 4-CP with uncalcined TiO₂-zeolite Y and calcined TiO₂-zeolite Y catalyst

3.4.1 Effects of catalyst load

The effect of catalyst load on the photocatalytic oxidation of phenol over TiO₂-zeolite Y was studied by using five different catalyst loadings of 0.2, 0.4, 0.6, 0.8 and 1.0 g L⁻¹. As the catalyst load was increased from 0.2 to 1.0 gL⁻¹, conversion of phenol increased from 64.0 to 85.0 %. With 2-CP and 4-CP, catalyst load was increased from 0.4 to 0.8, 1.2, 1.6 and 2.0 g L⁻¹ as conversion achieved was not significant with catalyst load < 0.4 g L⁻¹. The initial reactant concentration (phenol, 2-CP and 4-CP) was kept constant (0.2 × 10⁻³ M) and the reactions were carried out for a constant time interval of 300 min. A smooth increasing trend with increasing catalyst load was observed. With 2-CP, conversion increased from 58.3 to 76.0% and with 4-CP, conversion increased from 42.9 to 68.0% as the catalyst load was varied from 0.4 to 2.0 g L⁻¹. The results are presented in Fig.6.

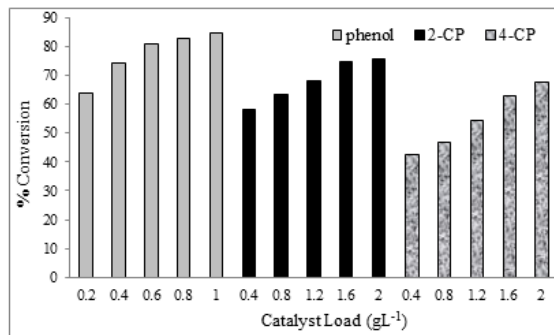


Fig.6. Effects of catalyst load on photocatalytic degradation of phenol, 2-CP and 4-CP over TiO₂-zeolite Y

It was observed in the present work that there was an increase in conversion at the initial stage, but the increase in the catalyst load beyond a certain value did not increase conversion. For example, with phenol, a sharp increasing trend was observed as catalyst load was increased from 0.2 to 0.6 g L⁻¹, increase in conversion became less rapid upto catalyst load 1.0 g L⁻¹. But when catalyst load was increased beyond 1.0 g L⁻¹, slight decrease in conversion was observed. The positive influence of increased catalyst load on solar photocatalytic conversion can be explained by the photocatalyst optical properties. The total active surface area increases with increasing catalyst load, because of the penetration of solar radiation into the reaction mixture, as a result of which the number of hydroxyl and superoxide radicals increases. The increased number of reactive centers generated by absorbed photons results in enhancement in the number of adsorbed reacting molecules, which in turn enhances the photocatalytic degradation [27].

However, beyond an optimal catalyst load, conversion decreases which can be attributed to the shielding (or shadowing) effect on the light. The number of adsorbed molecules does not further increase and the turbidity of the reaction mixture increases due to high catalyst load. As a result scattering of light takes place and penetration depth of solar radiation decreases [11, 28].

3.4.2. Effect of Initial reactant concentration

The photocatalytic conversion had shown a gradual decrease with increasing concentrations of phenol, 2-CP and 4-CP at a constant catalyst load of TiO₂-zeolite Y. As the initial concentration of phenol, 2-CP and 4-CP was increased from 0.2 × 10⁻³ M to 0.4 × 10⁻³ M, 0.6 × 10⁻³ M, 0.8 × 10⁻³ M and 1.0 × 10⁻³ M at a constant catalyst load (1.0 g L⁻¹ for phenol and 2.0g L⁻¹ for 2-CP and 4-CP), the conversion of phenol decreased from 85.0 to 81.0, 74.0, 67.1 and 66.0 %, 2-CP conversion decreased from 76.0 to 74.9, 71.0, 69.7 and 67.0% and 4-CP conversion decreased from 68.0 to 61.8, 57.0, 55.2 and 45.0% respectively. The results are presented in Fig. 7.

The decrease in conversion with increase in initial reactant concentration might be due to several factors such as saturation of active sites and the formation of intermediates on the surface of catalyst [29]. Moreover, the increased concentration affected penetration of solar radiation into the reaction mixture. At higher initial reactant concentration, fewer photons managed to reach the catalyst surface, as a result of which photocatalytic conversion was decreased.

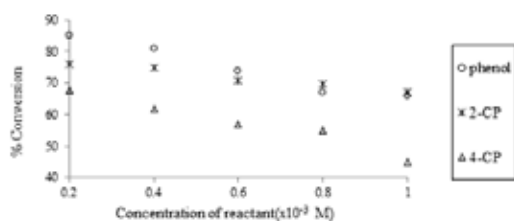


Fig.7. Effect of initial concentration on conversion of phenol, 2-CP and 4-CP over TiO₂-zeolite Y catalyst [Catalyst load 1.0 g L⁻¹ for phenol and 2.0g L⁻¹ for 2-CP and 4-CP, reaction time 300min]

3.4.3. Effect of pH of the medium

The effects of initial pH on the photocatalytic degradation of phenol, 2-CP and 4-CP over TiO₂-zeolite Y catalyst were studied within the pH range of 2.0 to 12.0. The results are presented in Fig. 8. It was observed that pH of the reaction medium played a significant role in the photocatalytic degradation of phenol, 2-CP and 4-CP.

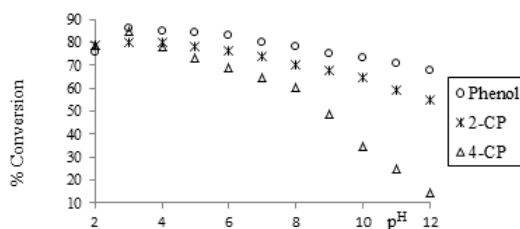


Fig. 8. Effects of pH on photocatalytic degradation of phenol, 2-CP and 4-CP over TiO₂-zeolite Y catalyst

An appreciable increase in conversion was observed for all the three phenolic compounds when the pH was in the lower side for all the catalysts. In case of phenol, as the initial pH was increased from 2.0 to 3.0, a sharp increase (by 10 %) in conversion was recorded. Maximum conversion was achieved at pH 3.0. Conversion slightly decreased when pH was increased upto 6.0, though the decrease was not very significant. With further increase in pH upto 12.0, the conversion decreased gradually. On the other hand, an overall decreasing trend was observed for both the chlorophenols as pH was increased from 2.0 to 3.0, and beyond pH 3, conversion decreased. Conversion of 4-CP was very little at pH beyond 10 and became negligible at pH 12.0. At the pH of the as-prepared aqueous solution of phenol, 2-CP and 4-CP (pH 4.5 for phenol, pH 6.34 for 2-CP, 6.12 for 4-CP), conversions achieved were 85.0%, 76.0% and 68.0 % respectively.

The influence of pH on the degradation of phenolic compounds may be attributed to competitive factors including the dissociation of phenol, the adsorption of OH⁻ and the adsorption of phenoxide ions [30]. The point of zero charge for TiO₂ is around pH 6.8 [31]. TiO₂ particles were thus positively charged at pH lower than 6.8, and were negatively charged above that pH. When the phenol solution is acidic, an attraction between TiO₂ photocatalyst and phenol molecules occurs and leads to an increase in the amount of phenol adsorbed on the positively charged surface of TiO₂ photocatalyst. For solutions of pH greater than 6.8, the groups with negative charge on the TiO₂ photocatalyst surface are likely to increase gradually. Thus low pH values can facilitate the adsorption of phenoxide ions on the surface of supported TiO₂ photocatalyst, which enhances phenol degradation.

At a very low pH such as 1.0, the surface of TiO₂ is occupied with H⁺ ions, and hence generation of OH[•] radical is retarded which in turn decreases conversion. High pH values favour the dissociation of phenol into phenoxide ion [30-32]. The phenoxide ion increases with increasing pH value and tend to replace the OH⁻ on the TiO₂ surface, which resulted in the reduction of OH[•] generation. Hence conversion decreased. The very low efficiency of the oxidation process of chlorophenols at pH > 10.0 could be explained with this reason since chlorophenol in alkaline medium is predominantly present as phenolate anion.

3.4.4. Effects of reaction time and kinetics of oxidation

It was found that the solar photocatalytic oxidation of phenol, 2-CP and 4-CP increased as the reaction time was increased from 15 to 300 min (Fig. 9).

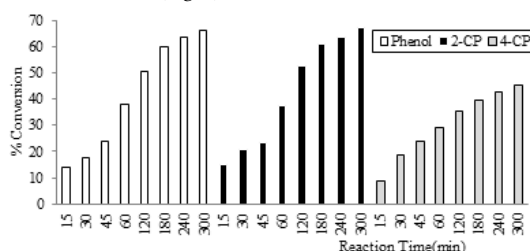


Fig. 9. Effects of reaction time on photocatalytic degradation of phenol, 2-CP and 4-CP over TiO₂-zeolite Y (reactant concentration 1.0×10^{-3} M, catalyst load: for phenol 1.0 g L⁻¹ and for 2-CP and 4-CP 2.0 g L⁻¹)

The apparent first-order rate coefficients of the reactions were obtained by plotting $\log C_t$ vs. time (Fig. 10) according to Lagergren pseudo first order kinetics. Very good linear plots were obtained for all the three reagents (regression co-efficient $R = 0.96 - 0.98$). The first-order rate coefficient, k_1 for solar photodegradation of phenol, 2-CP and 4-CP were calculated to be 4.4×10^{-3} , 3.9×10^{-3} and $2.1 \times 10^{-3} \text{ min}^{-1}$ respectively.

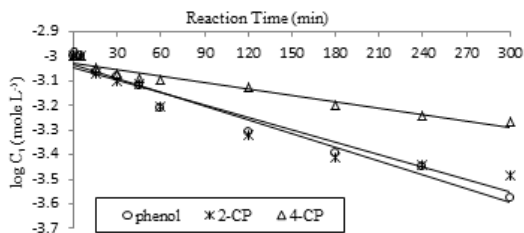


Fig.10. First-order kinetic plots of photocatalytic oxidation of phenol, 2-CP and 4-CP over TiO₂-zeolite Y

In the present work, the apparent first order rate constant was found to decrease with the increase in reactant concentration. This can be attributed to the increased number of intermediates generated during the photocatalysis at higher initial concentration of phenolic compounds[27]. The number of chlorine atoms present and their position on the aromatic ring had significantly different effects on the oxidation rate of chlorophenols. The degradability sequence of the phenol, 2-chlorophenol and 4-chlorophenol under study was: Phenol > 2-CP > 4-CP.

The effect of substitution of ring H by Cl on the aromatic ring on the degradability of chlorophenols is mainly caused by σ -electron withdrawing inductive effect, p-electron donating conjugative effect, and steric hindrance effect of chlorine [33]. The impact of steric hindrance effect of chlorine at ortho positions is more significant. The Cl at para position not only produced σ -electron withdrawing inductive effect but also might be dechlorinated when it was attacked by $\cdot\text{OH}$ radical. This markedly inhibited the oxidation reaction.

are easily available. Moreover, catalyst preparation is a simple process which makes it green alternative for treatment of polluted water. The degradation of pollutants using renewable solar energy is highly economical process compared with the processes using artificial UV radiation which require substantial electrical power input.

REFERENCE

- Legrini, O.; Oliveros, E.; Braun, A. M., (1993) Photochemical processes for water treatment, *Chem. Rev.*, 93,671-698. | 2. Blake, D. M., (1997) Bibliography of work on the photocatalytic removal of hazardous compounds from water and air, NREL/TP-430-22197, National Renewable Energy Laboratory, Golden Co. | 3. Herrmann, J.M., (1999) Heterogeneous photocatalysis: fundamentals and applications to the removal of various types of aqueous pollutants, *Catal. Today*, 53,115-129. | 4. Peral, J.; Domenech, X.; Ollis, D. F., (1997) Heterogeneous photocatalysis for purification, decontamination and deodorization of air, *J. Chem. Technol. Biotechnol.*, 70,117-140. | 5. Schiavello, M., (1987) (ed), *Photocatalysis and environment: trends and applications*, NATO ASI series C, vol 238. Kluwer Academic Publishers, London. | 6. Ollis, D. F.; Al-Ekabi, H. (1993) *Photocatalytic Purification and Treatment of Water and Air*; Elsevier: Amsterdam. | 7. Pellizzetti, E.; Minero, E.; Pramauro, C., In: Lasa HI, Dogu, G.; Ravella, A., (eds) (1993) *Chemical reactor technology for environmentally safe reactors and products*, Kluwer Academic Publishers, Dordrecht, The Netherlands, 77. | 8. Herrmann, J.M. (1999) In: Jansen F, van Santen RA (eds) *Water treatment by heterogeneous photocatalysis in environmental catalysis*, *Catalysis Science Series*, vol 1. Imperial College Press, London, Chapter 9, 171. | 9. Hoffmann, M. R.; Martin, S. T.; Choi, W.; Bahnemann, D.W., (1995) Environmental applications of semiconductor photocatalysis, *Chem. Rev.*, 95, 69-96. | 10. Ollis, D.; Pelizzetti, E.; Serpone, N., (1991) Photocatalyzed destruction of water contaminants, *Environ. Sci. Technol.*, 25,1522-1529. | 11. Nagaveni, K.; Sivalingam, G.; Hedge, M. S.; Madras, G., (2004) Solar photocatalytic degradation of dyes: high activity of combustion synthesized nano TiO₂, *Appl. Catal. B*, 48, 83-93. | 12. Brown, J. D.; Williamson, L. d.; Nozik, A. J., (1985) Moessbauer study of the kinetics of Fe³⁺ photoreduction on TiO₂ semiconductor powders, *J. Phys. Chem.*, 89, 3076-3080. | 13. Nagaveni, K.; Hegde, M. S.; Ravishankar, N.; Subbanna, G. N.; Madras, G., (2004) Synthesis and structure of nanocrystalline TiO₂ with lower band gap showing high photocatalytic activity, *Langmuir*, 20, 2900-2907. | 14. Xu, A. W.; Gao, Y.; Liu, H.Q., (2002) The preparation, characterization and their photocatalytic activities of rare-earth-doped TiO₂ nanoparticles, *J. Catalysis*, 207,151-157. | 15. Tang, J.; Wu, P.; Zheng, S.; Liu, Y.; Wang, F.; Xie, X., (2006) Synthesis and photocatalytic activity of Ti-pillared bentonite, *ACTA Geologica Sinica*, 80, 273-277. | 16. Zhu, H. Y.; Orthman, J. A.; Li, J.-Y.; Zhao, J.-C.; Churchman, G. J.; Vansant, E. F., (2002) Novel composites of TiO₂ (anatase) and silicate nanoparticles, *Chem. Mater.*, 14, 5037-5044. | 17. Choi, W.; Ko, J. Y.; Park, H.; Chung, J. S., (2001) Investigation on TiO₂-coated optical fibers for gas-phase photocatalytic oxidation of acetone, *Appl. Catal.*, B, 31, 209-220. | 18. Belhekar, A. A.; Awate, S. V.; Anand, R., (2002) Photocatalytic activity of titania modified mesoporous silica for pollution control, *Catal. Commun.*, 3, 453-458. | 19. Yoneyama, H.; Haga, S.; Yamanaka, S., (1989) Photocatalytic activities of microcrystalline TiO₂ incorporated in sheet silicates of clay, *J. Phys. Chem.*, 93, 4833-4837. | 20. Vinodgopal, K.; Hotchandani, S.; Kamat, P. V., (1993) Electrochemically assisted photocatalysis-TiO₂ particulate film electrodes for photocatalytic degradation of 4-chlorophenol, *J. Phys. Chem.*, 97, 9040-9044. | 21. Yoshida, H.; Kawase, T.; Miyashita, Y.; Murata, C.; Ooka, C.; Hattori, T., (1999) Effect of hydrothermal treatment of titania-pillared montmorillonite for photocatalytic degradation of dibutyl phthalate in water, *Chem. Lett.*, No.8, 715-716. | 22. Choi, W.; Hong, S. J.; Chang, Y.; Cho, Y., (2000) Photocatalytic degradation of polychlorinated dibenzo-p-dioxins on TiO₂ film under UV or solar light irradiation, *Environ. Sci. Technol.*, 34, 4810-4815. | 23. Tayade, R. J.; Kulkarni, R. G.; Jaska, R. V., (2007) Enhanced photocatalytic activity of TiO₂-coated NaY and HY zeolites for the degradation of methylene blue in water. *Ind. Eng. Chem. Res.*, 46, 369-376. | 24. Liu, X.; Iu, K.-K.; Thomas, J. K., (1993) Preparation, characterization and photoreactivity of titanium (IV) oxide encapsulated in zeolites *J. Chem. Soc., Faraday Trans.*, 89, 1861-1865. | 25. Corma, A.; Garcia, H., (2004) Zeolite-based photocatalysis, *Chem. Commun.*, (Cambridge), 1443-1459. | 26. Christidis, G. E.; Papantoni, H., (2008) Synthesis of FAU type zeolite Y from natural raw materials: hydrothermal SiO₂-sinter and perlite glass, *The Open Mineralogy Journal*, 2, 1-5. | 27. Laoufi, N. A.; Tassali, D.; Bentahar, F., (2008) The degradation of phenol in water solution by TiO₂ photocatalysis in a helical reactor, *Global NEST Journal*, 10, 404-418. | 28. Naik, B.; K. M. Parida, K. M., (2010) Solar light active photodegradation of phenol over a Fe_xTi_{1-x}O₂-yNy nanophotocatalyst, *Ind. Eng. Chem. Res.*, 49, 8339-8346. | 29. Sobczynski, A.; Duczmal, L.; Zmudzinski, W., (2004) Phenol destruction by photocatalysis on TiO₂: an attempt to solve the reaction mechanism, *J. Mol. Catal.*, A, 213, 225-230. | 30. Wei, T.-Y.; Wan, C.-C., (1991) Heterogeneous photocatalytic oxidation of phenol with titanium dioxide powders, *Ind. Eng. Chem. Res.*, 30, 1293-1300. | 31. Parra, S.; Sanca, S. E.; Guasaquillo, I.; Thampi, K. R., (2004) Photocatalytic Degradation of Atrazine Using Suspended and Supported TiO₂, *Appl. Catal. B*, 51, 107-116. | 32. Morrison, S. R., (1980) *Electrochemistry at Semiconductor and Oxidized Metal Electrodes*; Plenum Press: New York, Chapter 2. | 33. Zhang, J.; Li, G.B.; Ma, J., Effects of chlorine content and position of chlorinated phenols on their oxidation kinetics by potassium permanganate, (2003) *J. Environ. Sci.*, 15, 342-345. | 34. Debellefontaine, H.; Chakchouk, M.; Fousard, J.N.; Tissot, D.; Striolo, P., (1996) Treatment of organic aqueous wastes: Wet air oxidation and wet peroxide oxidation, *Environmental Pollution*, 92, 155-164.